

ARTICLE



Construction and validation of the diagnostic model of keloid based on weighted gene co-expression network analysis (WGCNA) and differential expression analysis

Jiaheng Xie^{a*} , Xiang Zhang^{b*}, Kai Zhang^{c*}, Chuyan Wu^d, Gang Yao^a, Jingping Shi^a, Liang Chen^e, Yiming Hu^f, Dan Wu^g, Guoyong Yin^h and Ming Wang^a

^aDepartment of Burn and Plastic Surgery, The First Affiliated Hospital of Nanjing Medical University, Nanjing, Jiangsu, China; ^bDepartment of Infection Management, The First Affiliated Hospital of Nanjing Medical University, Nanjing, Jiangsu, China; ^cPancreas Center, The First Affiliated Hospital with Nanjing Medical University, Nanjing, China; ^dRehabilitation Center, The First Affiliated Hospital of Nanjing Medical University, Nanjing, Jiangsu, China; ^eDepartment of General Surgery, Fuyang Hospital Affiliated to Anhui Medical University, Fuyang, Anhui, China; ^fCollege of Pharmacy, Jiangsu Ocean University, Lianyungang, Jiangsu, China; ^gDepartment of Rheumatology and Immunology, Nanjing Drum Tower Hospital, The Affiliated Hospital of Nanjing University Medical School, Nanjing, Jiangsu, China; ^hDepartment of Orthopaedics, The First Affiliated Hospital of Nanjing Medical University, Nanjing, Jiangsu, China

ABSTRACT

Keloid is a disease that seriously affects the aesthetic appearance of the body. In contrast to normal skin or hypertrophic scars, keloid tissue extends beyond the initial site of injury. Patients may complain of pain, itching, or burning. Although multiple treatments exist, none is uniformly successful. Genetic advances have made it possible to explore differences in gene expression between keloids and normal skin. Identifying the biomarker for keloid is beneficial to the mechanism exploration and treatment development of keloid. In this study, we identified seven genes with significant differences in keloids through weighted gene co-expression network analysis (WGCNA) and differential expression analysis. Then, by the Lasso regression, we constructed a keloid diagnostic model using five of these genes. Further studies found that keloids could be divided into high-risk and low-risk groups by this model, with differences in immunity, m6A methylation, and pyroptosis. Finally, we verified the accuracy of the diagnostic model in clinical RNA-sequencing data.

ARTICLE HISTORY

Received 7 September 2021
Revised 26 November 2021
Accepted 27 December 2021

KEYWORDS

Keloid; weighted gene co-expression network analysis; differential expression analysis; diagnostic model; RNA-sequencing

The pathological scar is a pathological product formed during the process of wound healing and is a hyperplastic disease of connective tissue in the skin [1]. Keloid is one of the common types of pathological scars and mostly occurred in colored race people [2]. It is usually manifested as a bulged, beyond the scope of the original wound, nodular hyperplasia, and a hard and reddish benign mass with itchy pain and discomfort [3]. Keloid is often accompanied by dysfunction, no degenerative changes, and tends to have aggressive growth [3]. The treatment effect is unwell for surgical excision alone since it is common to relapse after surgery [4]. Its effect on appearance and injury in the heart has a great negative impact on the living quality and mental health of patients.

The pathogenesis of keloid is complex, which is related to wound tension, genetic factors, immunological changes, programmed cell death, and other factors [5]. Previous studies have shown that the development of keloids is closely related to tumor-related genes [6]. Keloid is considered to be a benign fibrogenic skin tumor that includes many cancer-like characteristics, such as uncontrolled proliferation, lack of spontaneous recovery, and high recurrence rates [7]. Growing evidence suggests that various interactions promoting or inhibiting factors in tumors may explain the aggressive clinical behavior of keloids [8]. The most similar genotypes and phenotypes between keloid and cancer are

cellular energy sources, epigenetic methylation characteristics, and epithelial-mesenchymal transformation (EMT) behavior [9]. In this field, some tumor-related genes are included. These tumor suppressor genes: p53, Fas, P27, Rb Exon27, p16 lose their inhibitory effect on fibroblast proliferation after they mutated [9]. And the overexpression of c-myc, c-fos, and Tenascin-C can promote the proliferation of fibroblasts and inhibited cell apoptosis [10].

With the development of the public database of large-scale cooperative research, a large number of gene expression results from RNA-Seq were provided, including the keloid-related tissues. It provided great convenience for us to explore and identify the analysis of the differences in gene expression in keloid tissues. We downloaded the sequencing results related to keloid from the public database (GSE44270 and GSE145725) and integrated it. The study will contribute to a better understanding of the mechanism of keloid occurrence.

Methods

Recruitment of participants

The study was approved by the ethics committee of the First Affiliated Hospital of Nanjing Medical University (No. 2021-SR-418). All patients signed informed consent forms. A total of 3 keloid patients were recruited from the First Affiliated Hospital of

CONTACT Guoyong Yin  guoyong_yin@sina.com  wangming@jsh.org.cn

*These authors are the joint first authors.

Nanjing Medical University between February 2021 to August 2021. All patients underwent surgery to remove keloid tissue and surrounding 1 cm of normal skin. The keloid tissue was set as the disease group, and the paired normal skin was set as the control group, and RNA-sequencing was performed respectively. The clinical information of the three patients was summarized in Table 1.

Data processing

GSE44270 and GSE145725 were downloaded from the GEO database, and the robust multi-array average (RMA) algorithm was used for data homogenization and standardization. These two data sets were selected because of their large sample size and complete clinical features.

Weighted gene co-expression network analysis (WGCNA) in GSE44270 obtained the WGCNA-hub genes

The "WGCNA" R package was used to construct the co-expression network of all the genes in keloid and normal samples. Genes with the variance of up to 50% were screened for further analysis. The co-representation matrix was constructed by calculating the Pearson correlation coefficient. Then, we use the formula $amn = |cmn|^\beta$ (including amn : the adjacency relations between gene m and gene n , cmn : Pearson correlation coefficient, β : soft power threshold) weighted adjacency matrix is established. The weighted adjacencies matrix is transformed into a topological overlap measure matrix to estimate its connectivity in the network. The clustering tree of the matrix is constructed by means of average linkage

Table 1. Clinical characteristics of 3 patients.

Patient ID	Patient 1	Patient 2	Patient 3
Age	43	78	40
Gender	Female	Male	Female
area of the lesion	Chest	Left ear	Lower abdomen
Size (cm)	3 × 2	1.5 × 1.5	5 × 1

hierarchical clustering. Set the minimum gene module size to 30 to get the right module, and set the threshold for similar module merging to 0.25.

Differential expression analysis in GSE145725

After downloading the GSE145725 dataset, we homogenized and standardized the data. Then, differential expression analysis between keloid tissue and normal skin tissue was performed using the "Limma" package to obtain the differential expression genes ($|\log FC| > 1$ & $p < 0.05$). Subsequently, the "pheatmap" package was used to draw the expression heatmap, and the "ggplot2" package was used to draw the volcano map. Finally, the "clusterProfiler" package was used for GO enrichment analysis of differential genes to explore the function of DEG.

The intersection of WGCNA-hub genes in GSE44270 and DEGs in GSE145725 was used to obtain the 7 significant genes

In order to obtain the genes required for the construction of the keloid diagnostic model, we selected the intersection of WGCNA-hub genes in GSE44270 and DEGs in GSE145725. We use the "Venn" package in R software to draw and visualize Venn diagrams.

ROC curve analysis of 7 significant genes

The receiver operating characteristic curve (ROC) is a graph that reflects its diagnostic ability to recognize changes in threshold values. The closer the ROC curve is to the upper left corner and the larger the area under the curve (AUC) is, the better the diagnostic effect of this method is. We used the "pROC" package in GSE145725 to construct ROC curves for the seven modeled genes. Areas under the curve (AUC) can be compared using statistical tests based on U-Statistics or Bootstrap.

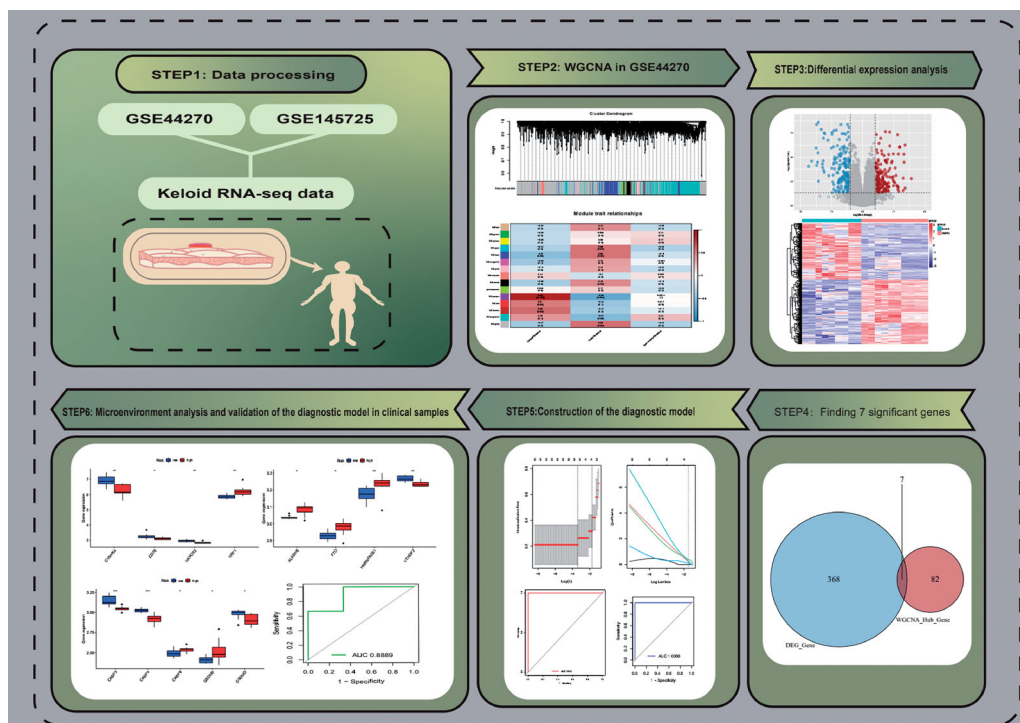


Figure 1. The flow chart of our study.

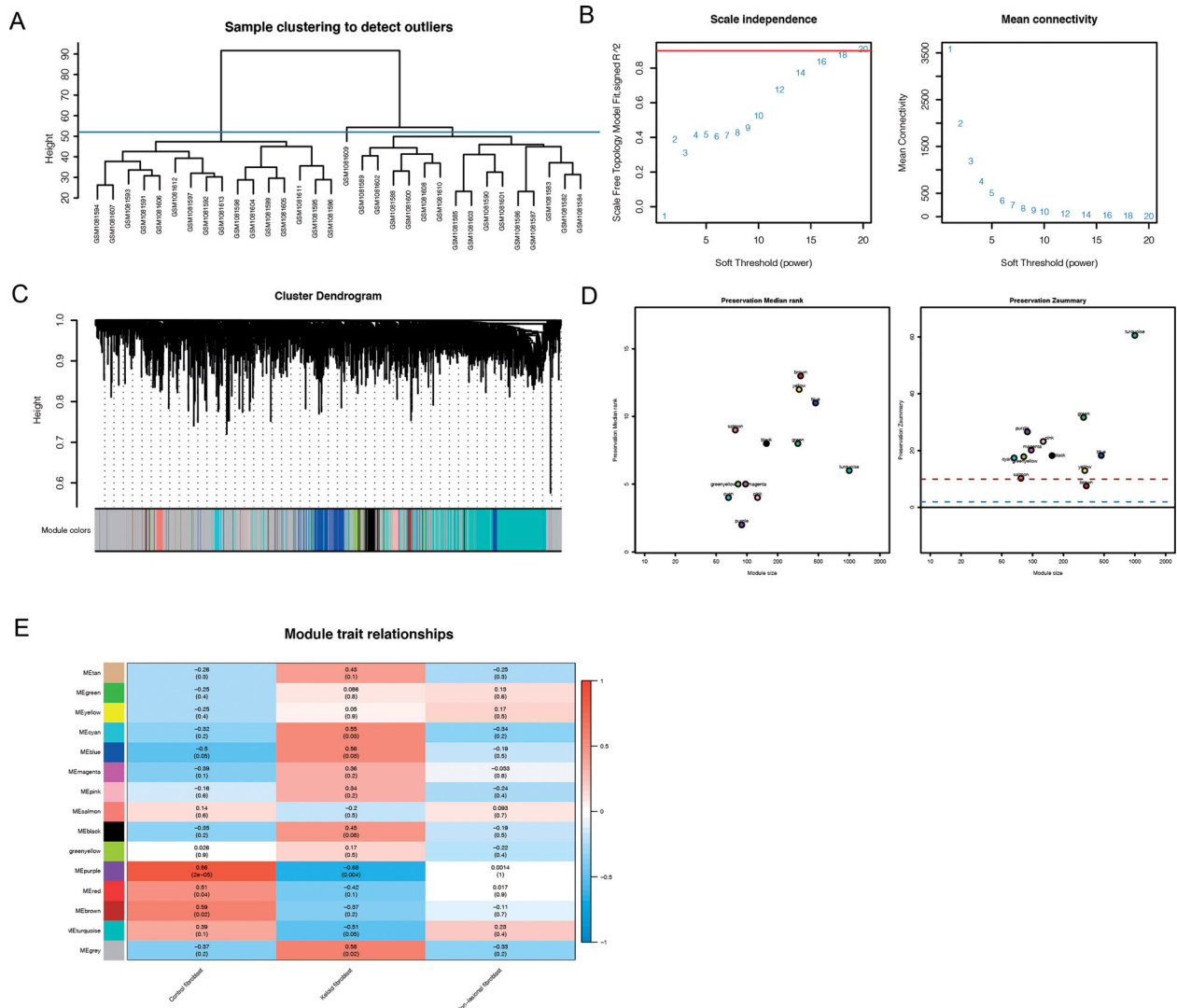


Figure 2. (A) By clustering these 32 samples, we found that the 16 samples on the left were quite different from the 16 samples on the right. After setting the truncation value of 55, we included the 16 samples on the left in the subsequent analysis. (B) As the threshold increased, the R_{02} value increased and crossed 0.8. We chose the optimal threshold of 18. (C) The turquoise module accounted for a larger proportion of the genes. (D) In order to verify the accuracy of the WGCNA process and results, the dataset was randomly divided into training set and testing set, and conservative sequences were identified and retained. Finally, the values of yellow, red and tan modules were found to be lower than 2, which were excluded. (E) Through correlation analysis between different modules and phenotype files, it was finally found that purple modules were significantly positively correlated with normal skin fibroblast (correlation = 0.86, $p < 0.001$), but significantly negatively correlated with keloid fibroblast (correlation = -0.68, $p < 0.01$). At the same time, there is no significant correlation in non-lesional fibroblast. The genes in the purple module were labeled as the WGCNA-hub genes.

The diagnostic model was constructed by lasso regression

We used the above 7 significant genes to conduct Lasso regression and construct the diagnostic model. Coefficients of selected features are shown by lambda parameter; Partial likelihood deviance versus $\log(\lambda)$ was drawn using the LASSO Cox Regression model. There were five genes that were significant after the Lasso regression. ROC curves of the diagnostic model were constructed in GSE44270 and GSE145725, respectively.

RNA sequencing to validate the diagnostic model

We recruited three patients to have keloids surgically removed by the same surgeon, and RNA-sequencing was performed on keloid specimens as well as the patients' normal skin (at least 10cm from the keloid lesion). TruSeq chain mRNA Library Prep Kit (Illumina) was used to generate the Library. Next-generation sequencing was performed on Illumina NovaSeq6000 (Illumina Inc., 100 cycles, single-read sequencing). Sample quality was

assessed by FastQC. Illumina NovaSeq6000 analyzed RNA sequencing data for more global analysis of genomic abnormalities. Data is preprocessed using standard pipelines that contain quality control indicators, such as FastQC and MultiQC. Sequence alignment based on STAR-RNA sequencer and sequencing reads allocated to genome features via Featurecots and Vomo-Transformed.

Immune, M6A methylation, and pyroptosis correlation analysis of the diagnostic model

We used the "ESTIMATE" package to calculate the immune score for each sample and then explored whether there were differences in immune scores between high- and low-risk groups. Then, immune checkpoint-related genes, m6A-related genes, and pyroptosis-related genes were extracted from previously published literature, and their expression matrices were compared between high- and low-risk groups.

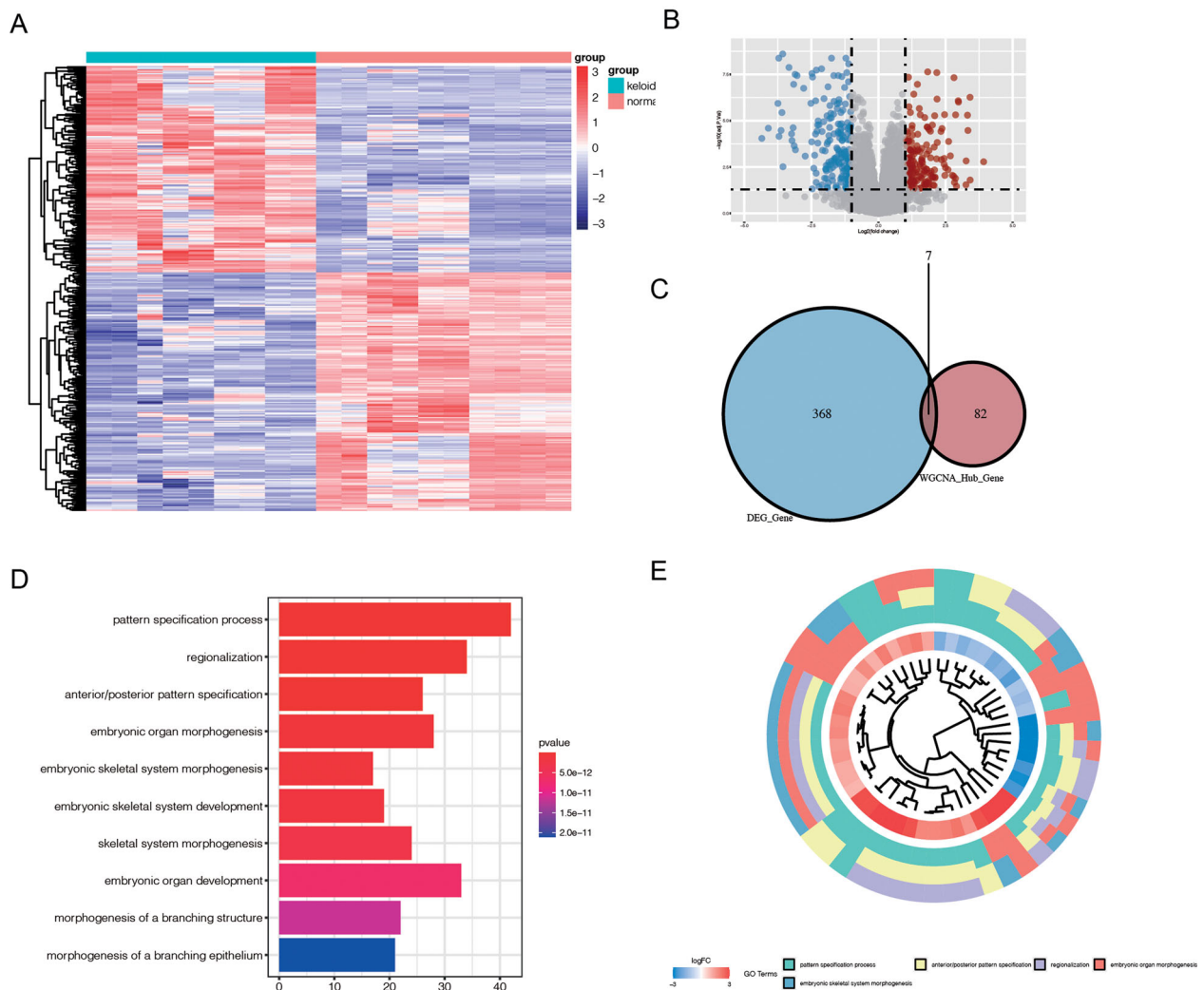


Figure 3. (A) The heat map shows the differential gene expression of keloids in GSE145725. (B) The volcano map shows the differential gene expression of keloids in GSE145725. (C) The 368 DEGs and 82 WGCNA-hub genes were intermingled, and 7 significant genes (FHL1, HOXA7, HOXC9, HSPA2, LOXL4, SKAP2, TNC) were obtained for the subsequent construction of diagnostic models. (D,E) Enrichment analysis found that DEGs was mainly related to pattern specification process, regionalization, anterior/posterior pattern specification, Organ morphogenesis, and other functions.

Results

Figure 1 shows a flow chart for data preparation, processing, analysis, and validation.

Weighted gene co-expression network analysis (WGCNA) in GSE44270

By clustering 32 samples in the dataset, we found that the 16 samples on the left and the 16 samples on the right were quite different and clustered into 2 clusters (Figure 2(A)). After setting the cutoff value to 55, we included the left 16 samples in the subsequent analysis. We found that as the threshold increased, the R^2 value increased and crossed 0.8 (Figure 2(B)). We chose the optimal threshold of 18. Then, we clustered similar genes into different modules, and the results showed that the turquoise module accounted for a larger proportion of the genes (Figure 2(C)). In order to verify the accuracy of the WGCNA process and results, the dataset was randomly divided into training set and testing set, and conservative sequences were identified and retained. Finally, the values of yellow, red and tan modules were found to be lower than 2, which were excluded, and the final findings were shown in Figure 2(D). Then, through correlation analysis between different modules and phenotype files, it was finally

found that purple modules were significantly positively correlated with normal skin fibroblast (correlation = 0.86, $p < 0.001$, Figure 2(E)), but significantly negatively correlated with keloid fibroblast (correlation = -0.68, $p < 0.01$, Figure 2(E)). At the same time, there is no significant correlation in non-lesional fibroblast, suggesting that the purple module plays an important role in scar fibers and normal fibers, which may be related to the occurrence and development of scar. The genes in the purple module were labeled as the WGCNA-hub genes.

Differential expression analysis in GSE145725

Through differential analysis, we found the differential expression of genes in keloids and normal tissues. Heat maps and volcanic maps show differential expression (Figure 3(A)). There were 368 differentially expressed genes (DEGs, Figure 3(B)). In order to further study the functional role of differential genes, we conducted GO enrichment analysis (Figure 3(D,E)). Enrichment analysis found that DEGs was mainly related to pattern specification process, regionalization, anterior/posterior pattern specification, Organ morphogenesis, and other functions (Figure 3(D,E)). The 368 DEGs and 82 WGCNA-hub genes were intermingled, and 7 significant genes (FHL1, HOXA7, HOXC9, HSPA2, LOXL4, SKAP2, TNC) were

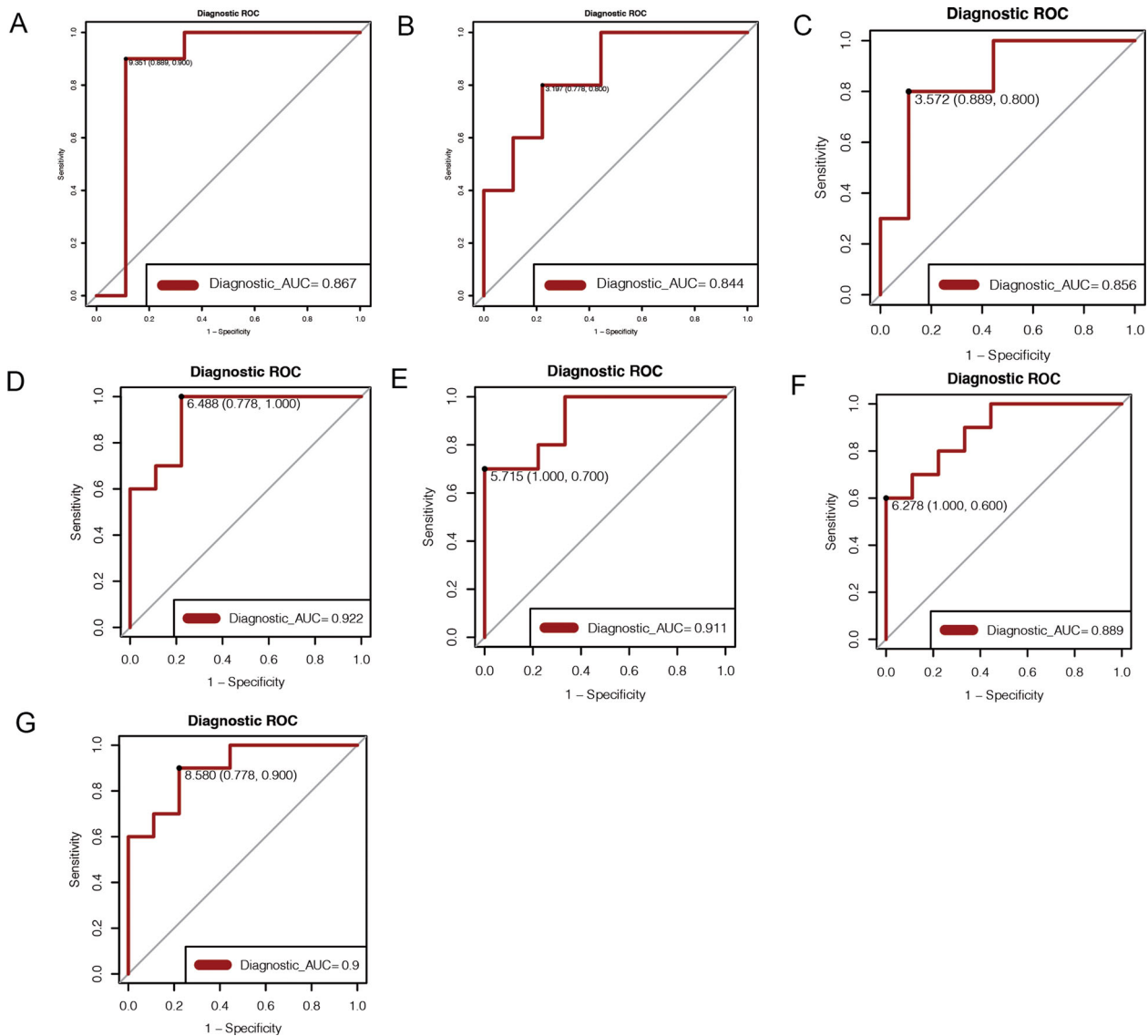


Figure 4. (A) ROC curve of FHL1 and the area under the curve is 0.867. (B) ROC curve of HOXA7 and the area under the curve is 0.844. (C) ROC curve of HOXC9 and the area under the curve is 0.856. (D) The ROC curve of HSPA2 and the area under the curve is 0.922. (E) ROC curve of LOXL4 and the area under the curve is 0.911. (F) The ROC curve of SKAP2 and the area under the curve were 0.889. (G) The ROC curve of TNC and the area under the curve was 0.9.

obtained for the subsequent construction of diagnostic models (Figure 3(C)).

Accuracy test of 7 significant genes

In GSE145725, ROC curves of these 7 significant genes (FHL1, HOXA7, HOXC9, HSPA2, LOXL4, SKAP2, TNC; Figure 4(A-G)) were plotted to test the accuracy of these 7 genes used in significant. By calculating the area under the curve (AUC), we can see the accuracy of the seven genes.

Construction of the diagnostic model in GSE145725

Lasso regression was performed on these 7 genes to construct the diagnostic model in GSE145725 (Figure 5(A,B)). Five of the genes (HOXA7, HSPA2, LOXL4, SKAP2, TNC) were found to be useful in diagnostic models. The risk scoring formula is: $\text{HOXA7} \times 0.1872975 + \text{HSPA2} \times 1.3501473 + \text{LOXL4} \times 1.1093921 + \text{SKAP2} \times 0.2883801 + \text{TNC} \times 1.7800625$. By median risk score (0.1339746), keloid patients were classified into high-risk and low-risk groups. The ROC curves of the diagnostic models were constructed in

GSE145725 (Figure 5(C)). We verified the ROC curve in GSE44270. The results showed that the AUC values were both 1 in GSE145725 and GSE44270, reflecting the accuracy of the models.

RNA sequencing to validate the diagnostic model

In our own sequencing data of 3 paired tissues from patients with keloid, the expressions of 7 significant genes were summarized in Table 2. We used the expressions of five of the significant genes to draw ROC curves to test the accuracy of the diagnostic model. The area under the ROC curve was 0.8889, indicating that the diagnostic model was valuable (Figure 6).

Immune, M6A methylation, and pyroptosis correlation analysis of the diagnostic model

We further explored the relationship between the diagnostic model and immunity, m6A methylation, and pyroptosis. First, we found that the high-risk group had higher immune scores than the low-risk group (Figure 7(A)). Secondly, we found low expression of three immune checkpoint-related genes in high-risk group:

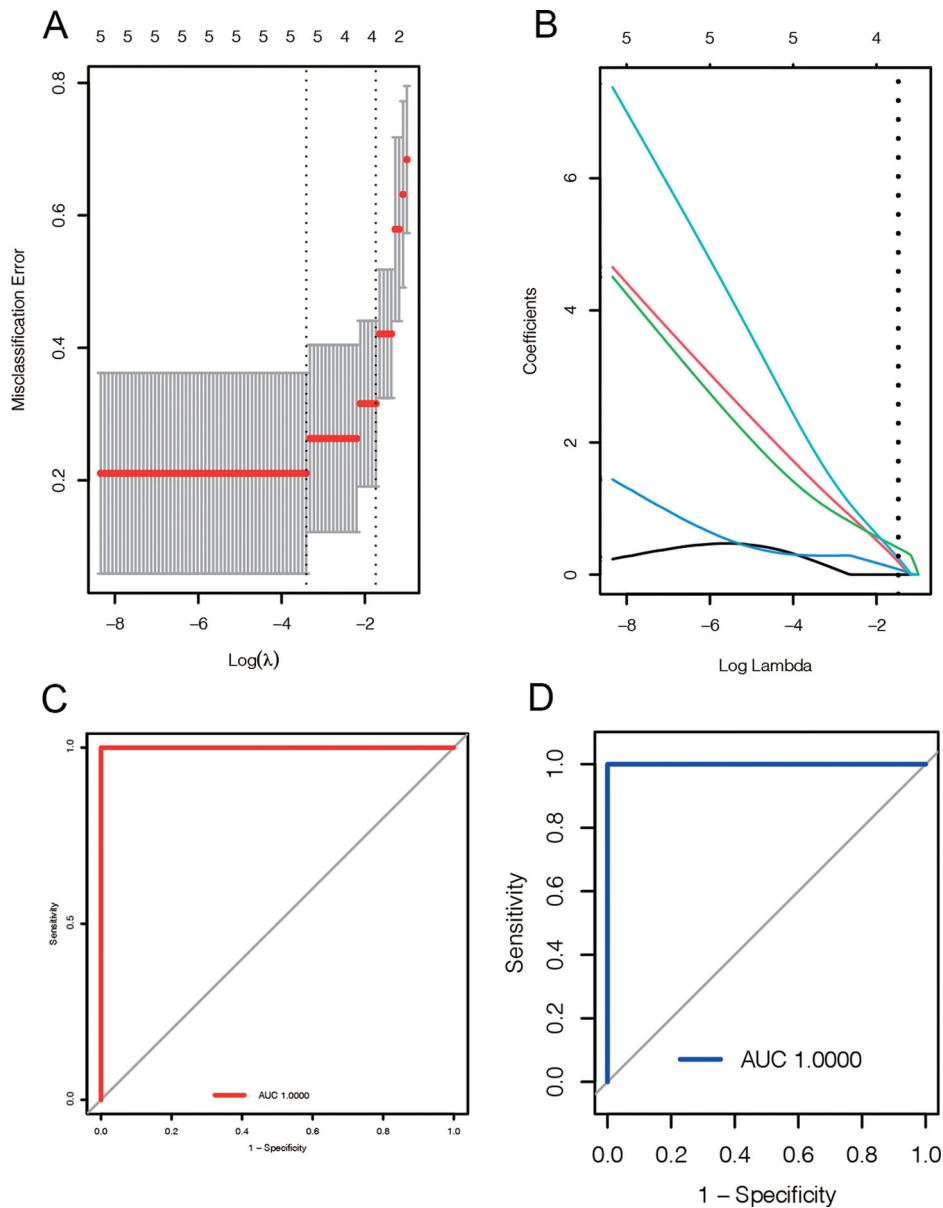


Figure 5. (A, B) Lasso regression was performed on these 7 genes to construct the diagnostic model. Five of the genes (HOXA7, HSPA2, LOXL4, SKAP2, TNC) were found to be useful in diagnostic models. (C, D) The ROC curves of the diagnostic models were constructed in GSE145725 (Figure 5(C)) and GSE44270 (Figure 5(D)), respectively. The area under the curve in both groups was 1.

Table 2. The expression of the 7 significant genes in keloids and normal tissues.

Gene name	Gene ID	p1_Keloid1 TPM	p1_Keloid2 TPM	p1_Keloid3 TPM	p1_Normal1 TPM	p1_Normal2 TPM	p1_Normal3 TPM
FHL1	2273	43.35	46.02	186.88	164.08	64.54	46.28
HOXA7	3204	2.19	3.84	0.1	4.66	8.23	7.1
HOXC9	3225	6.91	15.55	1.85	12.16	12.53	14.02
HSPA2	3306	13.65	18.46	12.58	35.38	24.97	28.82
LOXL4	84171	2.41	1.25	3.52	2.94	8.64	2.42
SKAP2	8935	10.55	12.68	4.92	14.44	8.1	10.4
TNC	3371	164.86	330.3	77.04	14.76	37.73	20.94

C10orf54, CD70, HAVCR2; A high expression of NRP1 in high-risk group (Figure 7(B)). Then, we explored differences in m6A methylation. Three genes, ALKBH5, FTO, and HNRNPA2B1, were highly expressed in the high-risk group, and one gene, YTHDF2, was lowly expressed in the high-risk group (Figure 7(C)). Finally, we investigated the relationship between diagnostic models and pyroptosis. The results showed that CASP8 and GSDMB were highly expressed in the high-risk group. Three genes related to

pyroptosis, CASP3, CASP4, and GSDMD, were low expressed in the high-risk group (Figure 7(D)).

Discussion

Keloid is a disease that seriously affects physical beauty. Its properties are similar to benign skin tumors with characteristics of abnormal accumulation of extracellular matrix and aggressive

growth [2]. With the development of society, the requirements for smooth and complete skin are also getting higher and higher, which not only requires functional recovery but also further

requires the aesthetic appearance [11]. Based on modern medicine, especially the deepening of basic research in cell biology, molecular biology, and gene genetics, the pathogenesis of keloid has been revealed gradually [10]. But keloid formation is a complex process with multiple mechanisms involved, and who is the initiating factor for this domino effect has yet to be identified [11]. More efforts are needed to study the mechanism and treatment of scar formation, and multi-therapy combination therapy is still a relatively recognized limited and safe strategy at present [1]. New technologies and treatments of trying might give the mechanism of scar brings new opportunities and perfect treatment research.

Chronic inflammatory environments have been shown to be a feature of keloids [1]. In addition, keloid has multiple hallmark traits of cancer, such as rapid cell proliferation, activation of growth signals, and reduced apoptosis [12]. This leads to the question of whether tumor therapies can be applied to keloids. At present, genome-wide association studies and epigenetics have greatly promoted the treatment of tumors, and disease treatment has gradually entered the era of precision medicine [13]. Therefore, similarly, identifying genetic differences between keloids and normal tissue makes sense to understand their pathogenesis and to develop a treatment based on this.

In this study, by weighted gene co-expression network analysis(WGCNA) in GSE44270 and differential expression analysis in GSE145275, we found seven genes with significant differences. After Lasso regression, five of the genes could be used to construct the diagnostic model of keloid. Then keloids samples in GSE44270 and GSE145275 can then be divided into high-risk and low-risk groups by calculating a risk score. We constructed the

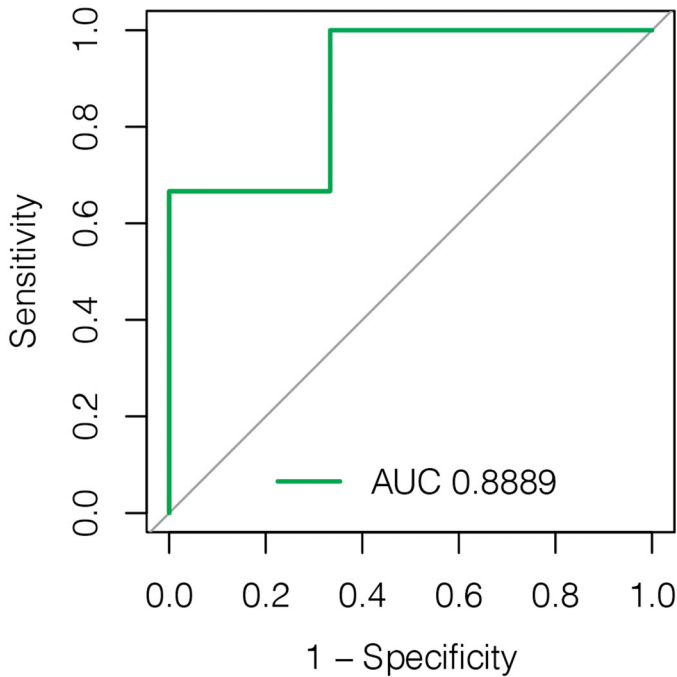


Figure 6. We used the expressions of five of the significant genes in clinical RNA-sequencing data to draw ROC curves to test the accuracy of the diagnostic model. The area under the ROC curve was 0.8889, indicating that the diagnostic model was accurate.

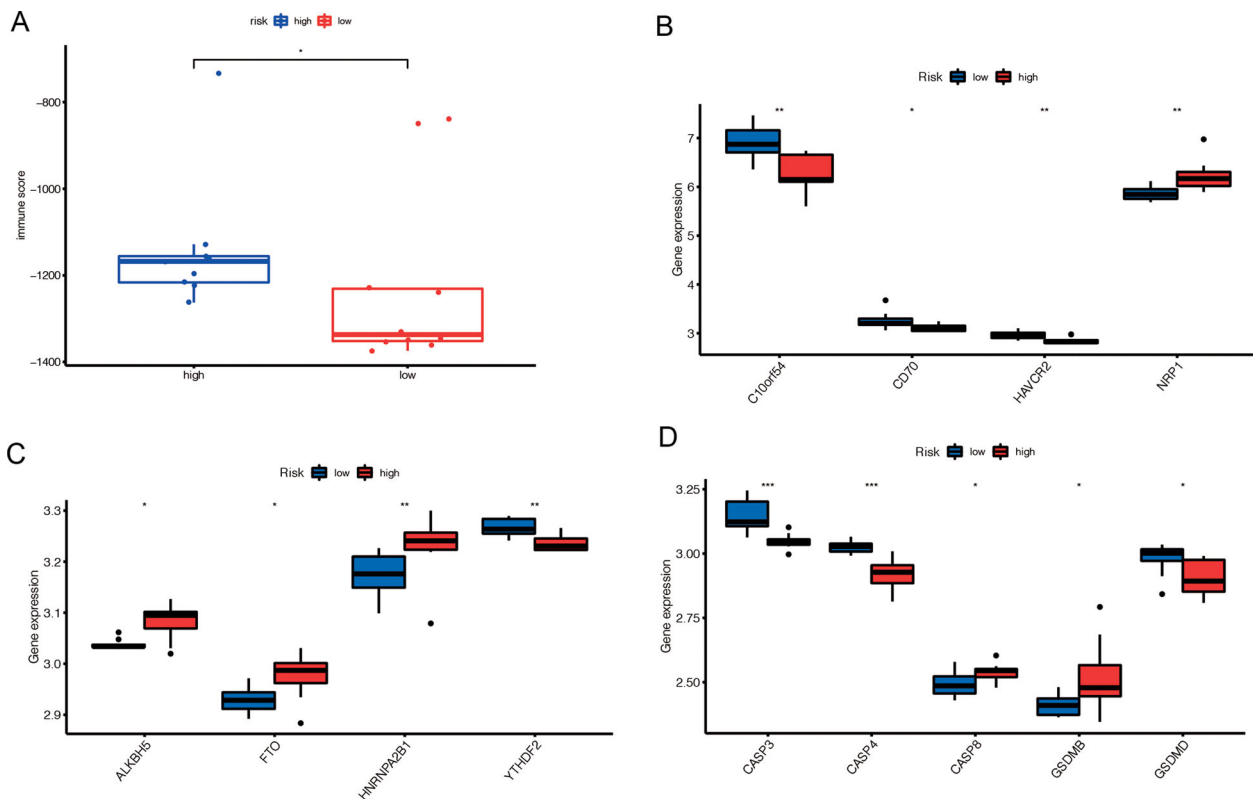


Figure 7. (A) The high-risk group had higher immune scores than the low-risk group ($p < 0.05$). (B) We found low expression of three immune checkpoint-related genes in high-risk group: C10orf54, CD70, HAVCR2; A high expression of NRP1 in high-risk group. (C) Three M6A methylation-related genes, ALKBH5, FTO, and HNRNP2B1, were highly expressed in the high-risk group, and one gene, YTHDF2, was lowly expressed in the high-risk group. (D) We investigated the relationship between diagnostic models and pyroptosis-related genes. The results showed that CASP8 and GSDMB were highly expressed in the high-risk group. Three genes related to pyroptosis, CASP3, CASP4, and GSDMD, were low expressed in the high-risk group. * $p < 0.05$, ** $p < 0.01$, and *** $p < 0.001$.

ROC curve of this diagnostic model in both two datasets and found that the accuracy of the diagnostic model was high after calculating the area under the curve (AUC), which is of further research value. Next, we explored the differences between the high-risk group and the low-risk group in the immune microenvironment, M6 methylation, and pyroptosis, and the results could provide some ideas for the pathogenesis of keloid. Finally, we tested the accuracy of the diagnostic model in the patient sequencing in our center and constructed the ROC curve. The area under the curve(AUC) showed that the accuracy of the diagnostic model was high.

Although the pathogenesis of keloid is still unclear, it is clear that chronic inflammatory response and infiltration of immune cells constitute the pathogenesis of keloid [1]. Various cytokines, such as interleukin 6, 8, 10, and growth factors, were found in high concentrations in keloids, which promoted our exploration of the mechanism of keloids [14]. In addition, it is important to explore the genetic changes in keloids, not only to help us understand their mechanisms but also to promote their treatment [15]. The diagnostic model we constructed can reveal a series of changes in keloid genesis from the perspective of genetics, and the new biomarkers can provide a basis for the development of future targeted therapy.

By dividing keloids into high-risk and low-risk groups, we were able to explore differences in their characteristics, which allowed us to target treatment and reduce unnecessary side effects. The higher immune scores in the high-risk group suggest that the infiltration of immune cells plays a greater role in their development, so this group of patients may benefit from immunosuppressive therapy. Similarly, m6A methylation differed between high- and low-risk groups. M6A is one of the most common post-transcriptional modifications and plays an important role in cancer and inflammatory diseases [16]. We found higher expression of m6A related genes in the high-risk group, which will help us to understand the mechanism of keloid and explore treatment options.

Cell pyroptosis is a form of programmed death that is gaining increasing attention and has been shown to play an important role in many proliferative diseases such as tumors [17]. The distinguishing feature of pyroptosis different from apoptosis is the release of inflammatory contents, which is involved in the formation of the inflammatory microenvironment of the disease [18–20]. Keloid is inflammatory hyperplasia [21]. Therefore, it is of great significance to explore the role of cell pyroptosis in keloid. We found differentially expressed genes related to cell pyroptosis in the high-risk group and the low-risk group, which provides some reference for subsequent studies.

In conclusion, our study provides a diagnostic model for keloid from the perspective of genetics, which provides some ideas for future gene therapy and targeted therapy for keloid. However, our study has limitations. We only validated the diagnostic model on sequencing data and lacked functional experiments of genes, which we will improve in the future.

Conclusion

We constructed a novel diagnostic model for keloids. Keloids can be divided into high-risk and low-risk groups according to this model. There were differences between the high-risk group and the low-risk group in immune score, immune-checkpoint, m6A methylation, pyroptosis, which provided ideas for the formulation of treatment regimens based on risk grouping. Moreover, we verified the accuracy of the diagnostic model in clinical samples.

Acknowledgments

We are very grateful for data provided by databases such as TCGA, GEO.

Ethical approval

All procedures performed were in accordance with the declaration of the ethical standards of the institutional research committee and with the 1964 Helsinki 387 Declaration and its later amendments. The ethics committee has approved this study of the First Affiliated Hospital of Nanjing Medical University (No. 2021-SR-418).

Disclosure statement

No potential conflict of interest was reported by the author(s).

ORCID

Jiaheng Xie  <http://orcid.org/0000-0002-4992-498X>

Data availability statement

GSE145275, GSE44270 in GEO database.

References

- [1] Ogawa R. Keloid and hypertrophic scars are the result of chronic inflammation in the reticular dermis. *IJMS*. 2017; 18(3):606.
- [2] Jones ME, McLane J, Adenegan R, et al. Advancing keloid treatment: a novel multimodal approach to ear keloids. *Dermatol Surg*. 2017;43(9):1164–1169.
- [3] Lee JY, Yang CC, Chao SC, Wong TW. Histopathological differential diagnosis of keloid and hypertrophic scar. *Am J Dermatopathol*. 2004;26(5):379–384.
- [4] LaRanger R, Karimpour-Fard A, Costa C, et al. Analysis of keloid response to 5-Fluorouracil treatment and long-term prevention of keloid recurrence. *Plast Reconstr Surg*. 2019; 143(2):490–494.
- [5] Mrowietz U, Seifert O. Keloid scarring: new treatments ahead. *Actas Dermosifiliogr*. 2009;100 Suppl 2 (Suppl 2): 75–83.
- [6] Ekstein SF, Wyles SP, Moran SL, et al. Keloids: a review of therapeutic management. *Int J Dermatol*. 2021;60(6): 661–671.
- [7] Atiyeh BS, Costagliola M, Hayek SN. Keloid or hypertrophic scar: the controversy: review of the literature. *Ann Plast Surg*. 2005;54(6):676–680.
- [8] Hsu KC, Luan CW, Tsai YW. Review of silicone gel sheeting and silicone gel for the prevention of hypertrophic scars and keloids. *Wounds*. 2017;29(5):154–158.
- [9] Tan S, Khumalo N, Bayat A. Understanding keloid pathobiology from a quasi-neoplastic perspective: less of a scar and more of a chronic inflammatory disease with cancer-like tendencies. *Front Immunol*. 2019;10:1810.
- [10] He Y, Deng Z, Alghamdi M, et al. From genetics to epigenetics: new insights into keloid scarring. *Cell Prolif*. 2017; 50(2):e12326.
- [11] Andrews JP, Marttala J, Macarak E, et al. Keloids: the paradigm of skin fibrosis –pathomechanisms and treatment. *Matrix Biol*. 2016;51:37–46.

- [12] Jumper N, Paus R, Bayat A. Functional histopathology of keloid disease. *Histol Histopathol.* 2015;30(9):1033–1057.
- [13] König IR, Fuchs O, Hansen G, et al. What is precision medicine? *Eur Respir J.* 2017;50(4):1700391.
- [14] Lee HJ, Jang YJ. Recent understandings of biology, prophylaxis and treatment strategies for hypertrophic scars and keloids. *IJMS.* 2018;19(3):711.
- [15] Wang ZC, Zhao WY, Cao Y, et al. The roles of inflammation in keloid and hypertrophic scars. *Front Immunol.* 2020;11:603187.
- [16] Qin Y, Li L, Luo E, et al. Role of m6A RNA methylation in cardiovascular disease (review). *Int J Mol Med.* 2020;46(6):1958–1972.
- [17] Fang Y, Tian S, Pan Y, et al. Pyroptosis: a new frontier in cancer. *Biomed Pharmacother.* 2020;121:109595.
- [18] Frank D, Vince JE. Pyroptosis versus necroptosis: similarities, differences, and crosstalk. *Cell Death Differ.* 2019;26(1):99–114.
- [19] Shi J, Gao W, Shao F. Pyroptosis: gasdermin-mediated programmed necrotic cell death. *Trends Biochem Sci.* 2017;42(4):245–254.
- [20] Kovacs SB, Miao EA. Gasdermins: effectors of pyroptosis. *Trends Cell Biol.* 2017;27(9):673–684.
- [21] Huang C, Liu L, You Z, et al. Managing keloid scars: from radiation therapy to actual and potential drug deliveries. *Int Wound J.* 2019;16(3):852–859.